

CHEMILUMINESCENCE OF DIPHENOYL PEROXIDE ELECTRON TRANSFER REVEALED BY LASER SPECTROPHOTOMETRIC ANALYSIS¹

KEITH A. HORN and GARY B. SCHUSTER*

Department of Chemistry, Roger Adams Laboratory, University of Illinois, Urbana, IL 61801, U.S.A.

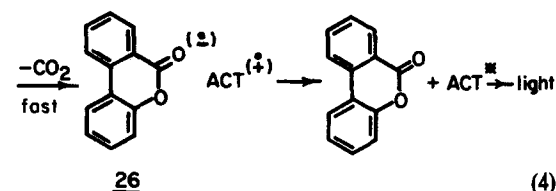
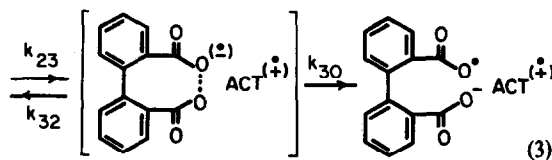
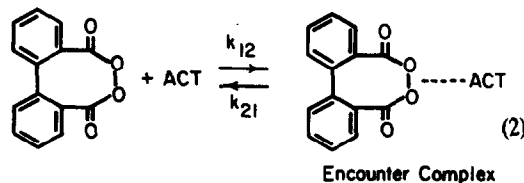
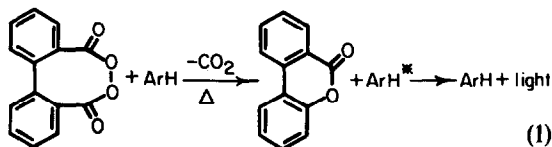
(Received in U.S.A. May 1981)

Abstract—The reaction of diphenoyl peroxide with a series of electronically excited electron donors was investigated by nanosecond laser spectroscopy. The results indicate that electron transfer from the excited state to the peroxide is the predominant reaction. The radical ions formed in this process may diffuse from the solvent cage or annihilate to regenerate the excited state. Kinetic data is presented that show an analogous process occurs for ground state electron donors resulting in chemiluminescence by the chemically initiated electron exchange luminescence (CIBEL) mechanism.

Chemiluminescence from the reactions of organic molecules requires the formation of electronically excited states. The generation of excited states of atoms and molecules has long been associated with electron transfer reactions. However, it has not been recognized until quite recently that single electron transfer reactions are central to many chemi- and bioluminescent transformations.² This circumstance is not unique. It is often difficult or impossible to decide if the bimolecular transformation of even-electron reactants into even-electron products passes through an intermediate odd-electron state or if it follows the more familiar closed-shell, two electron path. Discrimination between these two routes cannot be made by resort to analysis of the form of reaction kinetics, or by analysis of reaction stereochemistry. Often the evidence used to distinguish electron transfer from nucleophilic (or electrophilic) mechanisms of reaction is based on a correlation of the structure of the reactants with the rate of the reaction. Indeed, such a correlation provided the first evidence for the involvement of electron transfer in the chemiluminescence of organic peroxides. A less ambiguous method to assess the involvement of an intermediate odd-electron state in a reaction is to detect it directly. In some circumstances where the intermediate has high stability and builds up to a macroscopic concentration this can be done by conventional optical or electron resonance spectroscopy. In the more common circumstance where the lifetime of the intermediate is short, its detection can sometimes be accomplished using CIDNP techniques³ or by flash photolysis.⁴ The latter tool, especially when combined with a correlation of the structure of the reactants and reaction rate, can provide direct confirmation of the major participation of electron transfer in a chemical transformation. We report herein the application of laser flash photolysis to the analysis of the mechanism for the chemiluminescence observed from diphenoyl peroxide (DPP) in its reactions with certain aromatic hydrocarbons.

Thermolysis of DPP in a variety of solvents in the presence of any of several easily oxidized fluorescent hydrocarbons (ArH) generates CO₂, benzocoumarin and light, eqn (1).⁵ It has been shown by us that the ArH is a catalyst for the reaction, and that its catalytic effectiveness is predicated solely upon its one electron oxidation potential (E_{ox}). Other easily oxidized fluorescent compounds, such as amines and ethers, also catalyze the chemiluminescent reaction of DPP. These compounds

taken together are called catalytic chemiluminescent activators (ACT). The mechanism advanced to explain these, among other, observations is shown in Scheme 1 and is identified as chemically initiated electron-exchange luminescence (CIBEL). The first step in the proposed sequence is the diffusion together of the peroxide and activator to form an encounter complex. Thermal activation of this complex, resulting in a lengthening of the O–O bond and a concomitant lowering of the reduction potential of the peroxide, is postulated to initiate transfer of an electron from the activator to form the species, transition state or intermediate, shown in brackets in eqn (3).⁶ Rapid cleavage of the O–O bond in this species gives diphenate radical anion in a solvent cage with the activator radical cation. Loss of CO₂ and cyclization of the resulting anion gives, as nearest neighbors, benzocoumarin radical anion and activator radical cation. Well precedented annihilation of these



oppositely charged radical ions leads to electronically excited activator that is detected by its chemiluminescence. The key step in this sequence is the activated transfer of an electron from even-electron activator to even-electron peroxide to generate the postulated odd-electron intermediates. Subsequent rearrangement of the reduced peroxide serves to pump up the reducing potential of the transferred electron so that when it is returned to the activator sufficient energy is released to populate electronically excited states. Of course, this last step is not a prerequisite for this mechanism to operate, and non-chemiluminescent examples of this sequence have been suggested.⁷

The availability of high intensity, nanosecond, pulsed lasers has allowed us to probe in depth the reactions of DPP with electronically excited activators. We report here the unambiguous observation of radical ion intermediates on the CIEEL path with diphenoyl and phthaloyl peroxides, and the results of the investigation of the radical ion pairs generated in the CIEEL process.

RESULTS AND DISCUSSION

Photoexcitation of an aromatic hydrocarbon results in both an increase in its ability to act as an oxidant and in its ability to act as a reductant.⁸ Thus, electron-transfer reactions of excited state aromatic hydrocarbons in polar solvents have been observed to occur with electron donors (N,N-diethylaniline)⁹ as well as with electron acceptors (*p*-dicyanobenzene, tetracyanoethylene).¹⁰ In the present study of the CIEEL mechanism for the chemiluminescence of diphenoyl peroxide, advantage has been taken of the increased reducing power of singlet and triplet excited aromatic hydrocarbons in order to confirm the formation of the radical ion intermediates. Pulsed laser excitation has allowed detection of the radical ions by their characteristic absorption spectra and has provided a means to measure the rates of the electron-transfer processes involved.

The detection of radical ion intermediates

Pyrene singlet-diphenoyl peroxide. The fluorescence of excited singlet pyrene (Py*)¹ is quenched by DPP. This is evidenced both by a decrease in the pyrene fluorescence lifetime and a decrease in the pyrene fluorescence intensity in acetonitrile solution when DPP is added. The transient absorption spectrum measured 200 ns after nitrogen laser excitation of pyrene in the presence of diphenoyl peroxide in acetonitrile is shown in Fig. 1. It has a sharp maximum at 450 nm and is identical in all respects with the spectrum previously reported for pyrene radical cation.¹¹ No significant decay of the transient is observed during the first 500 ns following the laser excitation. This is consistent with the observed millisecond lifetime of pyrene radical cation in acetonitrile.¹² Furthermore, the transient absorption cannot be due to pyrene excited singlet ($S_1 \rightarrow S_n$, $\lambda_{\max} = 470$ nm)¹³ since the lifetime of pyrene singlet is only ca. 50 ns in the presence of 2×10^{-3} M diphenoyl peroxide.

The rate constant for the growth of the pyrene radical cation absorption is of the same magnitude as the rate constant for the decay of pyrene fluorescence, thus kinetically linking the observed formation of the pyrene radical cation with the fluorescence quenching by diphenoyl peroxide. Exact measurements of the rate constant for growth of the pyrene radical cation could

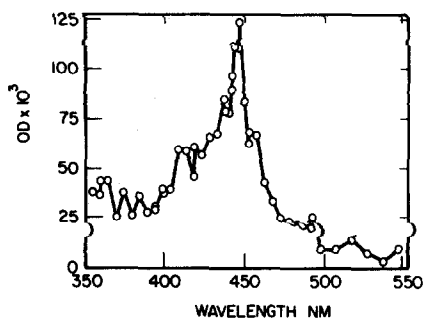
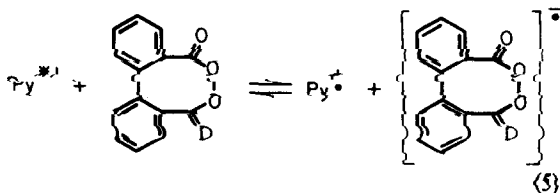


Fig. 1. The absorption spectrum of pyrene radical cation recorded 200 ns after laser excitation of pyrene in the presence of diphenoyl peroxide. The solvent is acetonitrile, the pyrene concentration is 3.04×10^{-5} M and the diphenoyl peroxide concentration is 2.40×10^{-3} M.

not be made due to the overlap of the pyrene fluorescence¹⁴ with the pyrene radical cation absorption.

The known propensity of excited singlet pyrene to act as a one-electron reductant in polar solvents, the known oxidizing ability of organic peroxides, and the observation of pyrene radical cation are, when taken together, highly suggestive of an electron-transfer mechanism for the fluorescence quenching of pyrene singlet by diphenoyl peroxide. The standard free energy change (ΔG) for such a process (eqn 5) can be calculated using eqn (6) provided that values for the oxidation potential of pyrene excited singlet and for the reduction potential of diphenoyl peroxide can be obtained. The oxidation potential of excited singlet pyrene can be estimated as the difference between the thermodynamic oxidation potential for ground state pyrene ($E_{\text{ox}} = 1.36$ V vs SCE)¹⁵ and its excited singlet energy (3.39 eV, 77 kcal/mol) or ca. -2.0 V vs SCE. The reduction potential of diphenoyl peroxide can be estimated to be ca. -0.1 – -0.4 V vs SCE, the typical range observed for the reduction potentials of diacyl peroxides as measured by polarography or cyclic voltammetry.¹⁶ This value is only an estimate because of the irreversibility of the electrochemical reduction of diacyl peroxides. Using these estimated values, the standard free energy for the electron-transfer reaction of pyrene singlet with diphenoyl peroxide (eqn 5) is calculated to be ca. -40 kcal/mol.

Two systems were used in direct comparison with the excited singlet pyrene-diphenoyl peroxide reaction. The first was the reaction of excited singlet pyrene with phthaloyl peroxide (PP).¹⁷ Laser excitation of pyrene in acetonitrile containing 2.51×10^{-3} M phthaloyl peroxide resulted in a transient absorption attributable only to pyrene radical cation. The standard free energy for electron transfer in this system is also estimated to be ca. -40 kcal/mol. The second system used for comparison with the diphenoyl peroxide was the reaction of *p*-

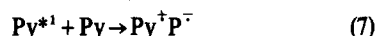


$$\Delta G = E_{\text{ox}} - E_{\text{red}} - \frac{e^2}{\epsilon R_0} \quad (6)$$

dicyanobenzene with excited singlet pyrene, a reaction shown previously by Weller^{10a} to proceed *via* an electron transfer to give pyrene radical cation and *p*-dicyanobenzene radical anion. The standard free energy change for the electron transfer from excited singlet pyrene to *p*-dicyanobenzene is estimated to be *ca.* -9 kcal/mol using eqn (6) and the known reduction potential of *p*-dicyanobenzene ($E_{\text{red}} = -1.65$ V vs SCE).⁸

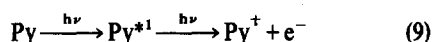
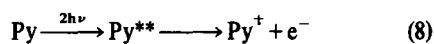
Association of the observed pyrene radical cation with the electron-transfer reaction of pyrene excited singlet with diphenoyl peroxide is predicated by the assumption that pyrene is not photoionized by laser excitation at 337 nm.

Photoionization of pyrene has been reported to occur in polar solvents (MeOH, MeCN, THF).¹⁸ Therefore, we undertook a series of experiments to determine the extent and mechanism of the photoionization of pyrene in acetonitrile and its relevance to the observed formation of pyrene radical cation in the presence of diphenoyl peroxide. These experiments revealed a slow appearance of pyrene radical cation in the absence of DPP which is consistent with either a bimolecular reaction of two pyrene triplet molecules to produce pyrene radical cation (observed in the laser photolysis of pyrene in THF)¹⁹ or an electron transfer from pyrene excited singlet (Py^{*1}) to pyrene ground state (eqn 7). This latter process has been substantiated by the recent work



of Watkins.²⁰ These mechanisms for the ionization of pyrene cannot be operative in the presence of diphenoyl peroxide because both pyrene singlet and pyrene triplet are quenched by the peroxide at rates near the diffusion limit.

Photoionization of pyrene has also been postulated to occur either by the simultaneous absorption of two photons (eqn 8) or by a consecutive biphotonic



process (eqn 9)²¹ under conditions of high energy laser excitation. However, pyrene excited singlet has not been

demonstrated to absorb at 337 nm. Moreover, the simultaneous two photon process (eqn 8) would predict a square dependence of the concentration of the pyrene radical cation on the nitrogen laser intensity. At the laser intensities used for the pyrene singlet-diphenoyl peroxide reaction this was not observed to be the case. Rather, the dependence of the optical density at 450 nm (λ_{max} of the pyrene radical cation) measured 50 ns after laser excitation was found to be linearly dependent on the laser intensity. In addition, little dependence of the optical density at 450 nm on the concentration of pyrene was observed. Therefore, we conclude that the pyrene radical cation observed in the presence of diphenoyl peroxide is produced by the reaction of diphenoyl peroxide with pyrene excited singlet (Py^{*1}).

The yield of cage-escaped pyrene radical cation (Py^{\dagger}) from each of the three systems studied (Py^{*1} -*p*-dicyanobenzene, Py^{*1} -phthaloyl peroxide, and Py^{*1} -diphenoyl peroxide) was estimated by measuring the optical density of its characteristic absorption 150 ns after the excitation when essentially all of the Py^{*1} has reacted, but well before there has been any significant reaction of the Py^{\dagger} . A comparison of the measured yields of Py^{\dagger} from these systems (Table 1) is particularly revealing. For the Py^{*1} -*p*-dicyanobenzene (DCB) system studied by Weller,^{10a} we have determined the yield of cage-escaped Py^{\dagger} to be 67% of the Py^{*1} that reacts with the DCB. The remaining 33% of the Py^{*1} is evidently converted to ground or triplet state pyrene, apparently by in-cage ion annihilation. The 48% yield of Py^{\dagger} measured from the reaction of phthaloyl peroxide (PP) with Py^{*1} is similar to that observed for the Py^{*1} -DCB system. In contrast to these cases, the reaction of Py^{*1} with diphenoyl peroxide in acetonitrile yields only *ca.* 5% cage-escaped Py^{\dagger} . It should be noted also, that in comparison to diphenoyl peroxide, phthaloyl peroxide is not chemiluminescent upon thermolysis with ground state aromatic hydrocarbons.²²

The CIEEL mechanism provides a convincing explanation for the different behavior of phthaloyl and diphenoyl peroxides. One-electron reduction of DPP by Py^{*1} followed by O-O bond cleavage generates diphenate radical anion. Subsequent rapid decarboxylation and ring closure of this radical anion produces benzocoumarin radical anion ($\text{BC}^{\cdot-}$), presumably within the same solvent cage as Py^{\dagger} . The radical ion pair $\text{Py}^{\dagger}\text{BC}^{\cdot-}$, can react by any of several energetically

Table 1. The quantum yields for the formation of pyrene radical cation by electron transfer from pyrene excited singlet to electron acceptors

Electron Acceptors	[] ^a	[Py] ^a	Trial	$\phi_{\text{Py}^{\dagger}}$ ^b
DCB	2.97×10^{-3} M	5.12×10^{-5} M	1	.66
			2	.69
PP	2.99×10^{-3} M	5.12×10^{-5} M	1	.46
			2	.50
DPP	3.00×10^{-3} M	5.12×10^{-5} M	1	.048
			2	.050

^aAll measurements were made at $23 \pm 2^{\circ}$ in nitrogen-purged acetonitrile solution. ^bThe optical density of the Py^{\dagger} absorption was monitored at 450 nm.

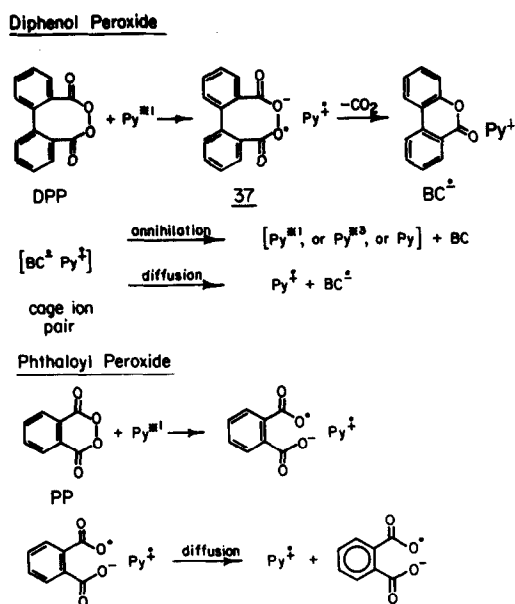
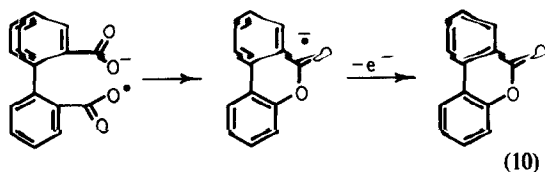


Fig. 2. Comparison of the electron-transfer reactions of phthaloyl and diphenoyl peroxides with pyrene excited singlet.

feasible reaction channels (Fig. 2). One available pathway is the annihilation of the ion pair within the solvent cage. The energy released by this annihilation can be estimated to be ca. 3.3 eV by subtracting the reduction potential of benzocoumarin (-1.9 V vs SCE) from the oxidation potential of pyrene (1.36 V vs SCE) and correcting for the coulombic stabilization energy of the ion pair (eqn 6).²³ The annihilation is therefore sufficiently exothermic to repopulate the excited singlet state of pyrene or to generate either pyrene triplet or pyrene ground state. In competition with annihilation, diffusion into the bulk solution generates the low yield of cage-escaped Py^{*2} that we observe. On the other hand, one-electron reduction of phthaloyl peroxide generates phthalate radical anion. The structure of this species precludes its efficient rearrangement to a strong reducing reagent analogous to benzocoumarin radical anion. The in-cage ion annihilation reaction of Py^{*2} with phthalate radical anion even to ground-state pyrene is endothermic. This conclusion is based on estimates of the oxidation potentials of benzoate and other simple carboxylates.²⁴ It also rests on the assumption that oxidation of the phthalate radical anion does not regenerate phthaloyl peroxide, but, rather, generates the diradical which would result from oxygen-oxygen bond homolysis of phthaloyl peroxide. Thus, diffusion competes effectively with in-cage reactions of the PP system, and a relatively high yield of cage-escaped Py^{*2} is observed.

Products of the reaction of pyrene excited singlet with diphenoyl peroxide

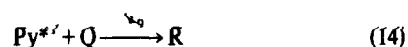
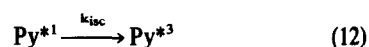
The only low molecular weight, volatile product from the reaction of diphenoyl peroxide and pyrene excited



singlet under the conditions of the laser photolysis is benzocoumarin. The 60% yield of benzocoumarin observed is similar to the yield of benzocoumarin from the thermal, ground state CIEEL reaction of diphenoyl peroxide with pyrene.⁵ The formation of benzocoumarin is readily explained by the decarboxylation of the diphenate radical anion which is formed by the initial electron transfer from pyrene excited singlet, followed by an electron transfer to some electron acceptor (e.g. Py^{*2}) (eqn (10)). However, no absorption attributable to benzocoumarin radical anion was detected in the transient absorption spectrum measured 140 ns after laser excitation of pyrene solutions containing diphenoyl peroxide. Attempts to generate independently benzocoumarin radical anion and to measure its absorption spectrum were unsuccessful. We can only conclude that the benzocoumarin radical anion is either of very short lifetime under the conditions of the laser photolysis or that it has no significant absorption in the wavelength region measured (perhaps due to a small extinction coefficient).

The kinetics of the quenching of pyrene fluorescence by diphenoyl peroxide

Confirmation of the idea that reactions of Py^{*1} with DPP can eventually regenerate Py^{*2} comes from an analysis of the kinetics of the fluorescence quenching reaction. Fluorescence quenching by any of the electron acceptors studied (DPP, PP, DCB) can be represented by the kinetic scheme shown in eqns (11)-(15), where Q is the quencher molecule, R represents the complex or radical ion pair formed by the quench, and k_n, k_{isc}, k_d and k_p are the



rate constants for fluorescence, intersystem crossing, radiationless deactivation, the quenching reaction, and the formation of products respectively. Since the intensity of fluorescence (I) is directly proportional to the concentration of Py^{*1}, analysis of the kinetic scheme leads to eqn (16). A plot of ln(I) vs time should yield a straight line with a slope proportional to (k_n + k_{isc} + k_d + k_q[Q]). Moreover, a plot of the quencher concentration

$$\ln(I) \alpha (-k_n - k_{isc} - k_d - k_q[Q])t \quad (16)$$

dependence of this complex rate constant should give the true quenching rate constant (k_q).

The situation is somewhat more complex if the radical ion pair which is generated is sufficiently energetic to regenerate Py^{*1} upon annihilation.



In this case a plot of $\ln(I)$ vs time would give a slope of

$$\text{Slope} = -k_n - \frac{k_p k_q}{k_p + k_{-q}} [Q]. \quad (18)$$

Similarly, a plot of the observed complex rate constant vs the concentration of the quencher should yield a slope equal to $k_p k_q / (k_p + k_{-q})$, a fraction times the true quenching rate k_q .

Typical pyrene fluorescence decay traces in acetonitrile both in the absence and presence of diphenoyl peroxide are shown in Fig. 3. The fluorescence decay both in the absence and presence of diphenoyl peroxide are pseudo-first-order in pyrene excited singlet as evidenced by a generally excellent fit of the intensity data to a first-order kinetic treatment. The same general characteristics were also observed for the quenching of pyrene fluorescence by phthaloyl peroxide and by *p*-dicyanobenzene. Plots of the dependence of the observed fluorescence rate constants in acetonitrile on the concentration of the added quencher (DPP, PP, or DCB) are linear and is shown for DPP in Fig. 4. The quenching rate constants extracted by a linear least-squares analysis of each of these sets of data are summarized in Table 2. The observed quenching rate constant for the reaction of *p*-dicyanobenzene with pyrene excited singlet in acetonitrile is close to the diffusion limited rate constant for this solvent²⁵ as is expected for an electron-transfer reaction that is exothermic by *ca.* -9 kcal/mol.²⁴ Similarly, electron-transfer from Py^{*1} to either DPP or PP is expected to occur at a diffusion limited rate since both processes are estimated to be exothermic by *ca.* -40 kcal/mol.

As is shown in Table 2, we have determined that phthaloyl peroxide reacts with pyrene excited singlet in acetonitrile with the diffusion limited rate constant of $(1.67 \pm 0.01) \times 10^{10} \text{ M}^{-1} \text{ S}^{-1}$. In contrast, diphenoyl peroxide reacts with pyrene excited singlet with an apparent rate constant of only $(1.02 \pm 0.007) \times 10^{10} \text{ M}^{-1} \text{ S}^{-1}$. This difference can be reconciled if, as we have suggested, pyrene excited singlet is regenerated to some extent from the in-cage, radical ion annihilation of pyrene radical cation with benzocoumarin radical anion but not from the pyrene radical cation-phthalate radical anion pair.

If the rate constant observed for the phthaloyl peroxide-pyrene excited singlet reaction is taken as the diffusion limited rate constant (k_q), then the extent of

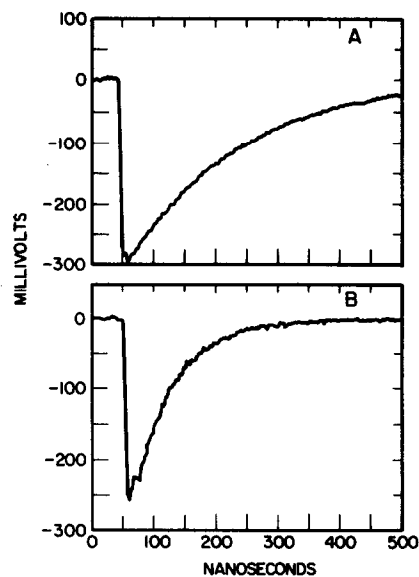


Fig. 3. Typical pyrene fluorescence decay in nitrogen-purged acetonitrile under conditions of added diphenoyl peroxide monitored at 390 nm. The pyrene concentration is $8.88 \times 10^{-5} \text{ M}$ and the diphenoyl peroxide concentration is 0 in A and $1.21 \times 10^{-3} \text{ M}$ in B.

pyrene singlet repopulation from the diphenoyl peroxide-pyrene excited singlet reaction is estimated to be 39%. This extent of repopulation of the pyrene excited singlet state is of the same magnitude as that observed pre-

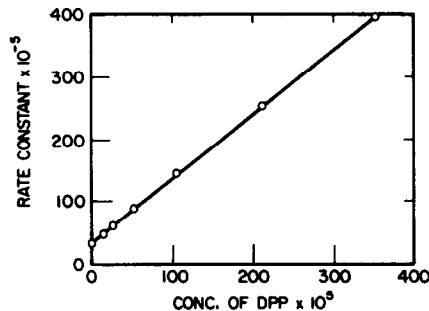


Fig. 4. Plot of the derived rate constants for pyrene fluorescence vs the concentration of added diphenoyl peroxide (DPP). The solvent is acetonitrile and the concentration of pyrene is $5.12 \times 10^{-5} \text{ M}$.

Table 2. The observed quenching rate constants for the quenching of pyrene fluorescence by various electron acceptors

Electron Acceptor	[Py]	Solvent ^a	Quenching Rate Constant ^b $\text{M}^{-1} \text{ S}^{-1}$
DPP	$5.12 \times 10^{-5} \text{ M}$	CH_3CN	$1.02 \pm (0.007) \times 10^{10}$
DPP	$8.88 \times 10^{-5} \text{ M}$	Et_2O	$1.14 \pm (0.04) \times 10^{10}$
PP	$5.12 \times 10^{-5} \text{ M}$	CH_3CN	$1.67 \pm (0.01) \times 10^{10}$
PP	$8.88 \times 10^{-5} \text{ M}$	Et_2O	$1.91 \pm (0.04) \times 10^{10}$
DCB	$5.12 \times 10^{-5} \text{ M}$	CH_3CN	$1.26 \pm (0.02) \times 10^{10}$
DCB	$5.12 \times 10^{-5} \text{ M}$	CH_3CN	$1.26 \pm (0.02) \times 10^{10}$

^aThe solutions were nitrogen-purged at 0° for 4 min. The fluorescence measurements were made at $23 \pm (2)^\circ$. ^bThe errors given are standard deviations.

viously for the chemiluminescent reaction of ground state pyrene with diphenoyl peroxide.⁵

The quenching rate constants for the reaction of pyrene excited singlet with diphenoyl and phthaloyl peroxides were also determined in diethyl ether. Here, the observed quenching rate constants for diphenoyl and phthaloyl peroxides increased by 12 and 14%, respectively, over the values measured in acetonitrile. This observed trend is consistent with the lower viscosity of diethyl ether. Interestingly, the extent of return to pyrene excited singlet in the diphenoyl peroxide case is also ca. 40%.

Quantum yield for the disappearance of peroxide

Pyrene excited singlet-diphenoyl peroxide. The quantum yield for the disappearance of peroxide in the reaction of DPP with pyrene excited singlet was measured to be 1.56 in N₂-purged acetonitrile. The quantum yield for the disappearance of peroxide for the reaction of phthaloyl peroxide with pyrene excited singlet similarly measured under laser photolysis conditions was found to be 0.81. If, as we have postulated, a CIEEL mechanism for the reaction of pyrene excited singlet with diphenoyl peroxide is operative, then the observed quantum yield for the disappearance of DPP is readily understood. The regenerated pyrene excited singlet from the pyrene radical cation-benzocoumarin radical anion annihilation can result in the destruction of a second diphenoyl peroxide molecule and thus propagate a short chain reaction. As expected, therefore, for the phthaloyl peroxide quench of pyrene excited singlet, where the radical ion pair cannot regenerate pyrene singlet, the quantum yield is observed to be less than one. However, a second explanation is feasible for the high quantum yield for the diphenoyl peroxide reaction. This postulated mechanism involves the reaction of cage-escaped benzocoumarin radical anion with diphenoyl peroxide. It would also provide a rational explanation for the lack of an absorption due to benzocoumarin radical anion in the transient absorption spectrum measured for the pyrene excited singlet-diphenoyl peroxide reaction. Our present experimental data do not allow us to distinguish between these two explanations of the high quantum yield for the diphenoyl peroxide system.

The interaction of diphenoyl peroxide with triplet excited state activators

To confirm the CIEEL mechanism for the reaction of diphenoyl peroxide with excited state aromatic hydrocarbons it was necessary to establish a correlation of the

rate constant for the reaction with the one-electron oxidation potentials of the excited states used. Extrapolation of the ground state diphenoyl peroxide chemiluminescence data⁵ to the oxidation potential of pyrene excited singlet would predict a bimolecular rate constant of $1.2 \times 10^{16} \text{ M}^{-1} \text{ S}^{-1}$. This impossibly large rate constant is considerably greater than the diffusion limited bimolecular rate constant we have observed for this reaction in acetonitrile. Therefore, we studied the reaction of diphenoyl peroxide with triplet excited state aromatic hydrocarbons. Generally, the oxidation potentials of the triplet states are considerably higher than that of pyrene excited singlet and are therefore expected to react with diphenoyl peroxide with rate constants substantially smaller than the diffusion limit.

We have measured the rate of reaction of the triplet states of anthracene, 9-acetylanthracene (9-AA), 9,10-dibromoanthracene (DBA), and fluoranthene with diphenoyl peroxide by monitoring the decay of their triplet-triplet absorptions following laser excitation. The decay of the triplet-triplet absorptions in the presence of DPP were generally pseudo-first-order in the triplet. Plots of the dependence of the observed rate constants for quenching of the various triplets on the concentration of added diphenoyl peroxide, shown in Fig. 5, give the quenching rate constants summarized in Table 3.

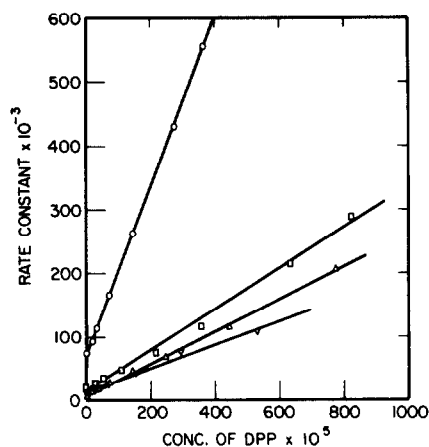


Fig. 5. Effect of increasing DPP concentration on the rate constants of decay of the triplet state electron donors. The data, in order of decreasing slopes correspond to fluoranthene, anthracene, 9,10-dibromoanthracene, and 9-acetylanthracene. The solvent is acetonitrile and the anthracene concentration is $3.93 \times 10^{-4} \text{ M}$.

Table 3. The observed quenching rate constants for the quenching of aromatic hydrocarbon triplets by diphenoyl peroxide

Aromatic Hydrocarbon	[ArH] ^a	E _{ox} [*] (V vs SCE)	E ^{*3} (kcal/mol)	E _{ox} ^{*3} (V vs SCE)	Peroxide	Quenching Rate Constant M ⁻¹ s ⁻¹
anthracene	$3.93 \times 10^{-4} \text{ M}$	1.37 ¹⁵	42.3	-.46	DPP	$1.44 \pm (0.03) \times 10^8$
9-AA	$5.26 \times 10^{-4} \text{ M}$	1.48 ^b	41	-.30	DPP	$2.65 \pm (0.07) \times 10^7$
DBA	$3.71 \times 10^{-4} \text{ M}$	1.38	40.2	-.36	DPP	$3.25 \pm (0.11) \times 10^7$
fluoranthene	$2.23 \times 10^{-4} \text{ M}$	1.73 ^c	52.9	-.55	DPP	$1.86 \pm (0.10) \times 10^8$

^aAll samples were prepared in acetonitrile and nitrogen purged for 4 min at 0° prior to the laser photolysis at $23 \pm (2)^\circ$. ^bMeasured by cyclic voltammetry in acetonitrile with $7.7 \times 10^{-2} \text{ M}$ tetra-*n*-butylammonium perchlorate as the supporting electrolyte. ^cThe oxidation potential for fluoranthene could not be measured due to experimental difficulties (see Experimental), therefore, the corrected value given by Parker¹⁵ was used.

Similarly, monitoring the rate of growth of the appropriate aromatic hydrocarbon radical cation gives identical rate constants. The rate data clearly do not correlate with the triplet energies of the aromatic hydrocarbons used. Rather, they correlate with the one-electron oxidation potentials of these excited-triplet states. The excellent correlation of these rate constants with the previously determined ground state activator rate data is shown in Fig. 6. This correlation demands that the rate-determining step for the ground and excited state reactions of diphenoyl peroxide with the various activators is the same, namely, electron transfer from the activator to the peroxide.

Transient absorption spectra of the aromatic hydrocarbon radical cations produced from these triplet quenching reactions establish further than an electron-transfer has taken place. The combination of these spectroscopic assignments and the kinetic correlation shown in Fig. 6 indicate that electron transfer to form odd-electron intermediates is the rate determining step in the strictly ground-state chemiluminescence of DPP. Thus, the mechanism identified as chemically initiated electron exchange luminescence is confirmed.

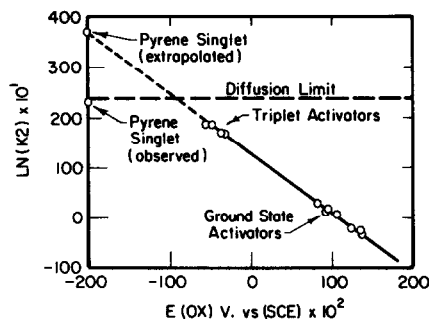


Fig. 6. Correlation of the reaction kinetics for the reaction of diphenoyl peroxide with ground and excited state activators. In order of increasing oxidation potential the points are: excited singlet pyrene, triplet fluoranthene, triplet anthracene, triplet 9-acetylanthracene, triplet 9, 10-dibromoanthracene, rubrene tetracene, triphenylamine, perylene, 9,10-diphenylanthracene, coronene, anthracene and pyrene.

CONCLUSIONS

The combination of kinetic, spectroscopic and structural experiments described above confirm the postulation of electron transfer as a key step in the chemiluminescence of DPP with ground and excited state aromatic electron donors. Moreover, the similar response of other chemi- and bioluminescent systems to the activators described herein suggests that many of these other systems behave analogously. This conclusion leads to the suspicion that many transformations of organic systems may be initiated by a similar activated electron transfer. The basic requirement for a mechanism such as this to operate is that oxidation (or reduction) of a substrate be irreversible due to a subsequent very rapid rearrangement. Back electron transfer then converts the odd-electron intermediate state to the even-electron products. The delineation of this mechanism in other than chemiluminescent systems awaits further investigation. However, the spectroscopic and kinetic tools we have described in this report should be widely applicable to these studies.

EXPERIMENTAL

General. $^1\text{H NMR}$ spectra were recorded on a Varian Associates EM-390 (90 MHz) or on a HR220 (220 MHz) instrument with TMS as the internal standard. UV absorption spectra were obtained with either a Cary 14 or a Beckman Acta MVI spectrometer. A Farrand Mark I spectrofluorometer was employed to record all emission and excitation spectra. Gas chromatographic analyses were carried out using a Varian Aerograph Model 2700 Chromatograph equipped with flame ionization detectors. Elemental analyses were performed by the Analyses Laboratory, Department of Chemistry, University of Illinois, Urbana, Illinois.

Pulsed nanosecond laser photolysis apparatus. The pulsed laser apparatus consists of a Molelectron Model UV 24 nitrogen laser (337.1 nm) having a 900 kW power rating at 20 Hz. The pulse width at half-height was typically of 10 ns duration and the baseline to baseline time resolution was 20 ns. The laser was mounted on a Newport Research Corporation optical table equipped with a pneumatic support system. The lensing system and physical arrangement of the detection equipment are shown in Fig. 7. Typically, the laser was focussed to a 3 mm \times 10 mm rectangle in the 1 cm sample cell. Power measurements of the laser pulse intensities (which varied generally between 2 and 7 mJ/pulse) were made at the sample table. Laser pulse intensities were typically reproducible to $\pm 5\%$.

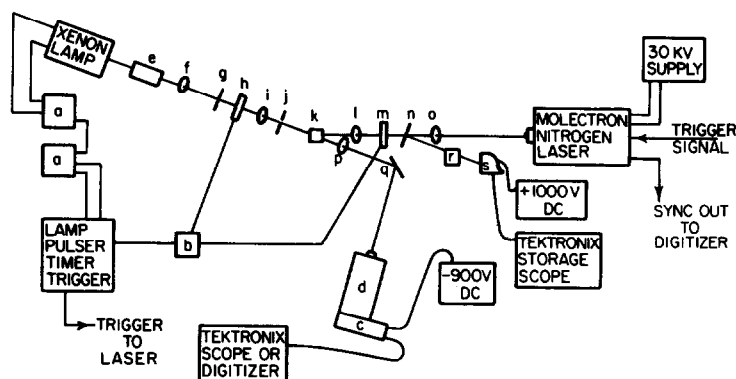


Fig. 7. Laser photolysis apparatus: a, PRA Model 301 Xenon arc lamp power supply; b, shutter control; c, Hamamatsu R928 photomultiplier tube; d, PRA Model 204B monochromator; e, PRA A1H1 IR filter; f, PRA Model LM-2 lens; g, 3 \times 10 mm aluminum slit; h, Uni Blitz Model 225 shutter; i, 38 mm dia. by 130 mm focal length lens; j, Schott glass filter WG345; k, translation stage sample table; l, 700 mm focal length AR-coated cylindrical lens; m, Uni Blitz Model 225 shutter; n, Quartz glass slide; o, 0.5 m focal length quartz lens; p, 38 mm dia. by 130 mm focal length lens; q, mirror; r, opal glass diffuser and neutral density filters; s, Hamamatsu Model vacuum photodiode.

The probe beam was generated by a PRA Model ALH 2150 450 W Xenon lamp operated at 20 amps and pulsed with a 60 μ F capacitor typically charged to 350 V. The probe light pulses thus generated were passed through both a PRA ALH 1 IR filter consisting of a water chamber and Schott glass filter 113 and a short wavelength UV filter consisting of the Schott glass filter WG 345 which were positioned before the sample table. The pulses were generally 140 μ s along (baseline to baseline) with a 2.5 μ s flat portion at the peak intensity. The total power of the probe pulse, measuring all wavelengths and integrated over the entire pulse, was determined to be $0.46 \pm 30\%$ mJ/pulse. A fast iris shutter (4 ms to full open) was placed between the xenon arc lamp and the cell to protect the sample from continuous irradiation by the probe light.

The probe light intensity and sample fluorescence were monitored using a Hamamatsu R928 photomultiplier tube with a 50 Ω termination. The tube was wired with a nonlinear, four-dynode chain to avoid space-charge problems and to prevent saturation at the higher light intensities used to overcome photon statistical noise. The high voltage DC power supply used was a Fluke Model 415 B. The rise time of the detector system (to -300 mV) was measured to be ca. 2 ns using a 30 ps green pulse generated by an argon ion laser. The recovery time of the tube was similarly measured to be ca. 1.5 ns. Saturation of the photomultiplier tube was found to occur at -350 – -400 millivolts as measured by insertion of neutral density filters into the pulsed probe beam. Thus, all absorption and fluorescence light intensities were adjusted to provide signals between 0 and -320 mV.

Spectral resolution was obtained using a PRA Model 204B monochromator which has a dispersion of 3.6 nm/mm. Thyatron noise was eliminated by using doubly-shielded coaxial cables for the power supplies and the detection system.

The measured absorption and fluorescence signals were processed using either a Tektronix 7834 storage oscilloscope (equipped with a differential comparator plug-in, 7A13 and the dual time-base 7B92A) or the Tektronix R 7912 transient digitizer. Both systems had time resolution capabilities of 0.5 ns. Most data was analyzed on the R 7912 which was interfaced to a Tektronix CP 4165 computer which was equipped with a CP 112 floppy disc unit and a 4010-1 graphics display terminal.

All measurements of the nitrogen laser intensity were made using a Gen Tec Joulemeter Model ED-200 7010 with a calibration of 6.50 V/J when terminated in 1 Meg Ω .

The sample cell used was a 1 cm square fluorescence cell which was fitted with a teflon stopcock and equipped with a small teflon-coated stir-bar.

Materials. *p*-Dicyanobenzene (Aldrich, 98%) was purified by recrystallization from ethanol. 9,10-Dibromoanthracene (Aldrich, 96%) was purified by multiple recrystallizations from acetonitrile. Fluoranthene (Aldrich, 98%) was first recrystallized from EtOH and then vacuum sublimed at 1.0 mm. Anthracene (Aldrich, 98%) was purified by mpic on silica gel (Ventron sieved silica gel, 45–60 μ 30 mm or by 75 mm column, eluant 20% CHCl_3 in hexane) followed by vacuum sublimation at 1.0 mm and 150°. 9-Acetyl-anthracene (Aldrich, 95%) was similarly purified by mpic chromatography on silica gel (eluant 35% CH_2Cl_2 in hexane) followed by recrystallization from EtOH and vacuum sublimation (1.0 mm) or alternatively by recrystallization from EtOH, vacuum sublimation and multiple recrystallization from EtOH. Pyrene (Aldrich, 99+%) was recrystallized from EtOH, purified by mpic on silica gel (5% CH_2Cl_2 in hexane) and then vacuum sublimed (0.4 mm, 100°). Acceptable elemental analysis were obtained for all compounds used.

Laser photolysis solvents. Acetonitrile (Aldrich spectrophotometric grade) was heated at reflux over CaH_2 and then distilled through a glass helix-packed, vacuum-jacketed, 76 cm vigreux column. A short forerun from each sample was discarded. The acetonitrile thus obtained showed no detectable absorption at 210 nm. Moreover, laser excitation (337.1 nm, ca. 5 mJ/pulse) of the sample cell containing only acetonitrile (N_2 -purged for 4 min) did not generate any detectable transients ($\text{OD} < 0.003$ from 350–750 nm) or any significant fluorescence or phosphorescence.

Diethyl ether (Baker analyzed reagent grade) was heated at

reflux over LAH and then distilled through a short vigreux column under nitrogen prior to use.

Absorption spectra of transient intermediates in the laser photolysis of pyrene. A 5 mL sample of a 6.8×10^{-5} M soln of pyrene in acetonitrile was placed in the laser photolysis cell and the N_2 purged for 4 min. The absorption spectra of the transient intermediates generated upon laser irradiation of this soln at 337 nm (laser intensity ca. 3 mJ/pulse) were measured 20 ns, 170 ns and 420 ns after the beginning of the laser pulse. Data were taken from 440 nm to 580 nm. The same process was repeated with a new sample of pyrene (6.8×10^{-5} M in CH_3CN , N_2 -purged) for an independent measurement of the absorption spectra of the transients at 100 ns, 800 ns and 1.6 μ s after laser excitation (laser intensity ca. 3.5 mJ/pulse).

The dependence of the optical density change at 450 nm (the λ_{max} of the pyrene radical cation absorption) on the laser pulse intensity was also measured. The nitrogen laser intensity was varied by inserting partially transmitting UV mirrors of known % transmittance calibration (50/50, 33/67) in the beam before the sample table. Next, the variation of the optical density at 450 nm with laser intensity for both a 6.8×10^{-5} M and a 3.4×10^{-5} M soln of pyrene in acetonitrile (each N_2 -purged for 4 min) was measured using the 50/50 and 33/67 mirrors singly and in combination. All optical density measurements for the laser excitation intensity dependence was made 50 ns after laser excitation.

Pyrene excited singlet—diphenoyl peroxide

Transient absorption spectrum. An acetonitrile stock soln of diphenoyl peroxide (2.40×10^{-3} M) containing pyrene (3.04×10^{-5} M) was prepared and held at 0°. Each 5 mL aliquot of this soln was placed in the laser photolysis cell and N_2 -purged at ambient temp for 3 min. Laser excitation of these samples (337 nm, ca. 2.5 mJ/pulse) generated readily observed pyrene fluorescence and a transient absorption which showed no significant decay in 500 ns. The absorption data (ΔOD) were measured 200 ns after laser excitation using the Tektronix 7834 storage scope. Measurement of the absorption at 200 ns avoided interference from pyrene fluorescence since the pyrene singlet lifetime was considerably shortened by the addition of diphenoyl peroxide. Absorption data were obtained from 350 to 555 nm with a spectral resolution better than 4 nm. The sample was agitated prior to each absorption measurement. The nitrogen laser was operated at 20 Hz and fast iris shutters were used to select the excitation pulse. The pyrene-diphenoyl peroxide samples were changed after every 6–7 points to prevent changes in concentration due to decomposition of the peroxide. The transient absorption upon excitation was monitored twice at 450 nm for each sample prepared. These consisted of the first and last data points taken with each sample. No decrease in the transient OD greater than the variation of the nitrogen laser pulse intensity ($\pm 8\%$) was observed. λ_{max} (of the transient) (CH_3CN) = 450 nm.

Anthracene triplet—diphenoyl peroxide

Quenching kinetics. A series of eight sample were prepared, each consisting of a 5 mL acetonitrile soln of anthracene (3.93×10^{-4} M) and containing various concentrations of diphenoyl peroxide (0 – 3.60×10^{-3} M). Each sample, in turn, was placed in the laser photolysis cell, N_2 -purged for 4 min and then photoexcited with the nitrogen laser (laser intensity ca. 2.7 mJ/pulse). The decay of the anthracene triplet absorption was monitored at 425 nm with a spectral resolution better than 4 nm. The strong fluorescence of anthracene caused the photomultiplier tube to saturate, especially at low concentrations of diphenoyl peroxide. Under these conditions, the photomultiplier tube recovery time was typically on the order of 0.8 μ s. Thus, the data for the anthracene triplet decay (collected with the R7912 transient digitizer) were analyzed from 1 μ s to 1.9 μ s after the laser excitation. The observed rate constant for the anthracene triplet decay was then calculated from the transient absorption data. Two trials for each sample were analyzed and averaged to obtain the rate constant for the triplet decay. A least squares analysis of the derived first-order triplet decay rate constants vs the concentration of added diphenoyl peroxide yielded the quenching rate

constant. Rate constants for the other triplet donors were obtained similarly.

Acknowledgements—We thank Mr. James Wetmer for his assistance in setting up the laser apparatus. This work was supported in part by the National Science Foundation and in part by the Office of Naval Research. GBS is a fellow of the Sloan and Dreyfus Foundations and KAH was a U of I fellow.

REFERENCES

- ¹A preliminary account of this work has appeared: K. A. Horn and G. B. Schuster, *J. Am. Chem. Soc.* **101**, 7097 (1979).
- ²J.-y. Koo, S. P. Schmidt and G. B. Schuster, *Proc. Natl. Acad. Sci. U.S.A.* **75**, 30 (1978).
- ³H. D. Roth and M. L. M. Schilling, *J. Am. Chem. Soc.* **102**, 4303, 7957 (1980).
- ⁴J. J. Zupancic, K. A. Horn and G. B. Schuster, *Ibid.* **102**, 5279 (1980).
- ⁵J.-y. Koo and G. B. Schuster, *Ibid.* **100**, 4496 (1978); *Ibid.* **99**, 6107 (1977).
- ⁶There has been some confusion regarding the legitimacy of this conclusion, C. Walling, *Ibid.* **102**, 1855 (1980). See, however, J. Scandola, G. Ditzian and G. B. Schuster, *Ibid.* **105**, (1983).
- ⁷See for example: L. Horner and E. Schwenk, *Angew. Chem.* **61**, 411 (1949).
- ⁸H. Schomburg, H. Staerk and A. Weller, *Chem. Phys. Lett.* **22**, 1 (1973).
- ⁹H.-J. Werner, H. Staerk and A. Weller, *J. Chem. Phys.* **68**, 2419 (1978).
- ^{10a}K. H. Grellmann, A. R. Watkins and A. Weller, *Ibid.* **76**, 469 (1972); ^bK. H. Grellmann, A. R. Watkins and A. Weller, *Ibid.* **76**, 3132 (1972).
- ^{11a}Z. H. Khan and B. N. Khanna, *Ibid.* **59**, 3015 (1973).
- ¹²K. H. Grellmann, A. R. Watkins and A. Weller, *J. Lumin.* **1**, 2, 676 (1976).
- ^{13a}S. Pantic and R. Zahradnik, *J. Phys. Chem.* **77**, 121 (1973).
- ^{13b}G. Porter and G. R. Tapp, *Nature* **228**, 228 (1968).
- ¹⁴I. B. Berlman, *Handbook of Fluorescence Spectra of Aromatic Molecules*, p. 383. Academic Press, New York (1971).
- ¹⁵V. D. Parker, *J. Am. Chem. Soc.* **98**, 98 (1976).
- ¹⁶O. Hammerich, *Encyclopedia of Electrochemistry of the Elements, Organic Section* (Edited by A. J. Bard), Vol. XI, pp. 316–340. Marcel Dekker, New York (1978).
- ¹⁷Phthaloyl peroxide was prepared by Dr. J. Zupancic by the method of Green: F. B. Green, *J. Am. Chem. Soc.* **78**, 2246 (1956).
- ^{18a}L. P. Gary, K. de Groot and R. C. Jarnagin, *J. Chem. Phys.* **49**, 1577 (1968); ^bS. D. Babenko and V. A. Bendersky, *Opt. Spectrosc.* **28**, 616 (1970); **29**, 45, 106 (1970).
- ¹⁹J. L. Metzger and H. Labhart, *Chem. Phys.* **7**, 150 (1975).
- ²⁰A. R. Watkins, *J. Phys. Chem.* **80**, 733 (1976).
- ²¹M. Ottolenghi, *Chem. Phys. Lett.* **12**, 339 (1971).
- ²²The report that phthaloyl peroxide generates singlet oxygen on *Quarodysis* (S. D. Dundermann and M. Staudert, *Angew. Chem.* (Int. Ed. Eng.), **14**, 560 (1975)) is in error.
- ²³D. Rehm and A. Weller, *Zur. J. Chem.* **8**, 259 (1970).
- ^{24a}L. Ebersson, *Acta Chem. Scand.* **17**, 2004 (1963); ^bM. J. Allen, W. G. Pierson and A. V. Celiano, *J. Electrochem. Soc. Japan*, **E30**, 30 (1962).
- ²⁵The diffusion limited rate constant for acetonitrile at 23° is estimated to be $ca. 1.7 \times 10^{10} M^{-1} S^{-1}$ by the Stokes-Einstein equation if a viscosity of $ca. 3.5$ millipoise is used for acetonitrile.